Groundwater contaminant flux reduction resulting from nonaqueous phase liquid mass reduction

J. W. Jawitz,[1] A. D. Fure,[2] G. G. Demmy,[3,4] S. Berglund,[5] and P. S. C. Rao[6]

Received 18 November 2004; revised 9 June 2005; accepted 23 June 2005; published 13 October 2005.

[1] This work presents a stream tube–based analytical approach to evaluate reduction in groundwater contaminant flux resulting from partial mass reduction in a nonaqueous phase liquid (NAPL) source zone. The reduction in contaminant flux, R_j, discharged from the source zone is a remediation performance metric that has a direct effect on the fundamental drivers of remediation: protection of human health and the environment. Closed form expressions are provided for analyzing remediation performance under conditions of joint spatial variability of both groundwater flow and NAPL content. The performance measures derived here are expressed in terms of measurable parameters. Spatial variability is described within a Lagrangian framework where aquifer hydrodynamic heterogeneities are characterized using nonreactive travel time distributions, while NAPL spatial distribution heterogeneity can be similarly described using reactive travel time distributions. The combined statistics of these distributions are used to evaluate the relationship between reduction in contaminant mass, R_m, and R_j. A portion of the contaminant mass in the source zone is assumed to be removed via in situ flushing remediation, with the initial and final conditions defined as steady state natural gradient groundwater flow through the contaminant source zone. The combined effects of aquifer and NAPL heterogeneities are shown to be captured in a single parameter, reactive travel time variability, which was determined to be the most important factor controlling the relationship between R_m and R_j. It is shown that as heterogeneity in aquifer properties and NAPL spatial distribution increases, less mass reduction is required to achieve a given flux reduction, although the overall source longevity increases. When rate-limited dissolution is important, the efficiency of remediation, in terms of both mass and flux reduction, is reduced. However, at many field sites the combined effects of field-scale heterogeneities and site aging will result in favorable relationships between mass reduction and flux reduction.

Citation: Jawitz, J. W., A. D. Fure, G. G. Demmy, S. Berglund, and P. S. C. Rao (2005), Groundwater contaminant flux reduction resulting from nonaqueous phase liquid mass reduction, *Water Resour. Res.*, *41*, W10408, doi:10.1029/2004WR003825.

1. Introduction

[2] Sites contaminated with dense nonaqueous phase liquids (DNAPLs) present significant challenges to the successful selection and implementation of remedial designs. There are two general approaches for managing the risk associated with DNAPL sites. The first approach is to manage or contain the dissolved plume emanating from the site, thereby isolating it from potential contaminant receptors. Plume management strategies can be generalized as containment (e.g., physical barriers), in situ methods (e.g., bioremediation), or removal (e.g., pump and treat). The major disadvantage of plume management approaches arises from the longevity of most DNAPL source zones, which tend to function as long-term sources of contamination under natural flowing groundwater conditions, translating to substantial operation and management costs. The persistence of DNAPLs in the subsurface makes the second risk management approach, contaminant source zone removal, an attractive option.

[3] Recent field applications of aggressive source zone remediation technologies have demonstrated the ability to remove or destroy a large portion of the contaminant mass [*Fountain et al.*, 1996; *Rao et al.*, 1997; *Jawitz et al.*, 1998b; *Martel et al.*, 1998; *McCray and Brusseau*, 1998; *Falta et al.*, 1999; *Lowe et al.*, 1999; *Fiorenza*, 2000; *Jawitz et al.*, 2000; *Meinardus et al.*, 2002; *Brooks et al.*, 2004]. In each of these studies, the analyses of remediation performance focused on the mass removal effectiveness of the remedial technology. However, in none of these studies was the contaminant mass completely removed. This trend has led to recent analyses [*Sale and McWhorter*, 2001] and subsequent debate [*Rao et al.*, 2001; *Rao and Jawitz*, 2003; *McWhorter and Sale*, 2003] regarding the merits of aggres-

[1]Soil and Water Science Department, University of Florida, Gainesville, Florida, USA.
[2]Department of Environmental Engineering Sciences, University of Florida, Gainesville, Florida, USA.
[3]Layton Graphics, Inc., Atlanta, Georgia, USA.
[4]Now at TerraGo Technologies, Marietta, Georgia, USA.
[5]Swedish Nuclear Fuel and Waste Management Company, Stockholm, Sweden.
[6]School of Civil Engineering, Purdue University, West Lafayette, Indiana, USA.

0043-1397/05/2004WR003825

sive source zone remediation. *Sale and McWhorter* [2001], who conceptualized the source zone as a network of discrete subzones of idealized geometry in a uniform flow field, concluded that near complete removal of the source zone mass is required to achieve meaningful improvements in groundwater quality. *Rao and Jawitz* [2003] suggested that any quantification of the benefits of source zone remediation should consider field-scale heterogeneities, and that the reduction in contaminant flux discharged from the source zone should be used as a performance metric in favor of strictly considering reduction in either total contaminant mass or groundwater concentration within the source zone. *Rao et al.* [2001] also argued for the latter point, proposing that, in a risk-based framework, a remedial technology (or combination of technologies) should be evaluated based on the ability to reduce the contaminant flux or mass discharge from the source zone to the dissolved contaminant plume to a level where the risk to down-gradient contaminant receptors is lowered below a certain threshold. However, despite the large body of recent work devoted toward aggressive source zone remediation technologies, an evaluation of these technologies in a risk-based paradigm is problematic because virtually all previous work has focused on mass reduction performance metrics and has not quantified the associated reduction in flux. This has been in part due to a historical dearth of reliable flux measurement methods [*U.S. Environmental Protection Agency* (*USEPA*), 2003]; however, at least two innovative flux measurement methods have recently emerged [*Bockelmann et al.*, 2001; *Hatfield et al.*, 2004], suggesting the potential for future flux-based site management decisions.

[4] The work presented here is an extension of *Rao and Jawitz* [2003] and *Parker and Park* [2004], who suggested that a continuum of relationships exist between contaminant mass and flux depending on the site-specific NAPL distribution, groundwater velocity field, and correlation between the two. This paper presents analytical relationships between NAPL mass reduction, R_m, and contaminant flux reduction, R_j, in terms of parameters that are measurable from nonreactive and reactive tracer tests. These closed form expressions enable the analysis of remediation performance under conditions of aquifer hydrodynamic heterogeneity, NAPL source zone heterogeneity, and nonequilibrium dissolution.

2. Problem Description

2.1. General Configuration

[5] This analysis focuses on the NAPL source zone, rather than the down-gradient aqueous dissolved plume. The problem description is similar to that described by *Berglund* [1997] where the source zone boundary conditions consist of two planes oriented orthogonal to the mean direction of natural flowing groundwater. The up-gradient plane, referred to as the injection plane, is located at $x = 0$ in the mean flow direction and consists of an array of injection wells through which remedial fluids are introduced. Likewise, the down-gradient plane, referred to as the extraction plane, is located at x_1 and consists of an array of extraction wells through which remedial fluids are extracted. A portion of the contaminant mass in the source zone is assumed to be removed via in situ flushing remediation. The initial and final conditions are defined as steady state natural gradient groundwater flow through the contaminant source zone, with groundwater velocities low enough that the NAPL source is in equilibrium with the water and the aqueous NAPL constituent concentration corresponds to the aqueous solubility limit, C_w [ML^{-3}]. The contaminant mass flux, or mass flow per unit area, J [$ML^{-2}T^{-1}$], is measured at the extraction plane during natural gradient groundwater flow.

[6] The aquifer hydraulic conductivity is assumed to be heterogeneous, resulting in a spatially variable velocity field that is represented here within a Lagrangian framework as a collection of noninteracting stream tubes. Each stream tube is characterized by a single travel time, and pore-scale dispersion is assumed to be negligible such that nonreactive transport is described as an advection-only process. Each stream tube initially contains immobile NAPL and the stream tube bundle collectively represents a contaminant source zone. Each stream tube may contain a different amount of contaminant, resulting in a spatial distribution of NAPL saturations. Thus aquifer hydrodynamic heterogeneities are characterized by a distribution of nonreactive travel times, while NAPL spatial distribution heterogeneity may be similarly described using reactive travel time distributions, with stream tube average sorption and dissolution reaction parameters that represent the integral effects of transport along a stream tube [*Cvetkovic et al.*, 1998; *Jawitz et al.*, 2003a]. The combined statistics of these distributions are used to evaluate the relationship between NAPL mass removal and reduction in down-gradient contaminant flux. An advantage of the Lagrangian approach is that the stream tube average nonreactive and reactive travel time distributions may be obtained from tracer tests, as described by *Jawitz et al.* [2003a].

[7] A stream tube is considered ''clean'' when all of the NAPL has been removed, and the aqueous contaminant concentration is then set equal to zero. As the remedial process progresses, an increasing number of stream tubes become clean. Thus, during source zone remediation, the fraction of stream tubes that are uncontaminated increases with remedial process duration, T. Partial, or incomplete remediation of the source zone is represented as the complete removal of contaminant mass from only a portion of the stream tubes with partial mass removal from the remaining portion. The statistics of the reactive travel time distribution that characterize the NAPL spatial variability are also a function of T. These effects are quantified here by considering incomplete, or truncated forms of the nonreactive and reactive travel time distributions where the truncation point is a function of T. The statistics of these truncated distributions are evaluated using truncated moment expressions presented by *Jawitz* [2004].

2.2. Simplifying Assumptions

[8] In the stream tube approach employed here, all fluids and solutes displaced through the domain are assumed to follow the same collection of streamlines. Thus the remedial fluids injected and extracted under forced gradient conditions are assumed to follow the same flow paths, resulting in the same nonreactive travel time distribution, as the natural gradient groundwater flow. Such conditions would apply for line drive well configurations oriented in the same direction as the mean natural gradient groundwater flow, or where the separation distance between injection and extraction planes is sufficient to minimize the effects of flow convergence and divergence around the wells. Examples of

other processes that may result in different fluids or solutes traveling along different streamlines include displacement instabilities induced by buoyant or viscous effects [*Jawitz et al.*, 1998a], transient flow due to time-varying boundary conditions such as seasonal shifts in hydraulic gradient [*Rivett and Feenstra*, 2005], temporal changes to the internal structure of the flow field such as relative permeability changes during NAPL dissolution [*Geller and Hunt*, 1993], and nonadvective transport (e.g., solutes with different effective diffusion coefficients [*Cirpka and Kitanidis*, 2000]). Here it is assumed that flow is stable and steady, advection is the dominant transport process, and NAPL saturations are generally low enough that dissolution will not significantly affect the flow field.

[9] While laboratory studies have demonstrated that local-scale transverse mixing is important for the dissolution of NAPL pools [*Chrysikopoulos et al.*, 2000; *Eberhardt and Grathwohl*, 2002], *Berglund and Fiori* [1997] determined that an advection-only approach is appropriate for describing the transport of sorbing solutes under typical field conditions. Furthermore, the numerical simulations of surfactant-based DNAPL source zone remediation of *Lemke et al.* [2004] found contaminant mass recovery and mass flux to be insensitive to transverse dispersivity values ranging from 0.0075 to 0.06 m, values extending well beyond the upper limit reported in field and laboratory experiments [*Klenk and Grathwohl*, 2002]. Thus, while other investigators have evaluated the importance of incorporating diffusion and other processes that cause differential mixing for different solutes into stream tube formulations [*Cirpka and Kitanidis*, 2000; *Ginn*, 2001], these effects were not specifically evaluated here.

[10] *Rivett and Feenstra* [2005] estimated a 20% reduction in porous media permeability due to the emplacement of a DNAPL source zone at a global saturation of 0.05. However, two studies at actual contaminated sites have reported average DNAPL saturations within the source zone of 0.004 to 0.009 [*Jawitz et al.*, 2000; *Meinardus et al.*, 2002]. Using the standard quartic relation between NAPL saturation and relative permeability cited by *Rivett and Feenstra* [2005], these low DNAPL saturations correspond to permeability reductions of less than 4%.

[11] In summary, the assumptions that advection is dominant over other processes such as diffusion, and that changes in relative permeability during NAPL dissolution do not substantially alter the flow field are not expected to severely limit the application of the methods and findings presented here. However, specific investigation of these effects is left for future work.

3. Stochastic-Advective Approach to Solute Transport

[12] Solute transport through porous media has been successfully modeled using the lognormal distribution to represent both nonreactive and reactive travel time distributions [e.g., *Jury and Roth*, 1990; *Demmy et al.*, 1999; *Jawitz et al.*, 2003b]. If solute arrival time, t, is considered as a random variable, then the lognormal probability density function (PDF), $p(t)$, is described by

$$p(t) = \frac{1}{\sqrt{2\pi}\sigma_{\ln t} t} \exp\left(-\frac{(\ln(t) - \mu_{\ln t})^2}{2\sigma_{\ln t}^2}\right) \qquad t > 0,\ \sigma_{\ln t} > 0 \tag{1}$$

where $\mu_{\ln t}$ and $\sigma_{\ln t}$ are the mean and standard deviation of the normal distribution $Y = \ln t$.

3.1. Truncated Moment Expressions

[13] The Nth absolute moment of a probability distribution, $p(t)$, is defined as

$$m_N^t = \int_{-\infty}^{\infty} t^N p(t) dt \tag{2}$$

A truncated or incomplete distribution is one where data are unavailable above or below some upper or lower truncation point, $t_{\min}$ and $t_{\max}$. The Nth truncated moment for an incomplete distribution is defined [*Jawitz*, 2004] as

$$m_N^t(t_{\min}, t_{\max}) = \int_{t_{\min}}^{t_{\max}} t^N p(t) dt \tag{3}$$

Note that the moments of the complete distribution are special cases of the truncated moments with $m_N^t(-\infty, \infty)$. However, for brevity the familiar notation m_N^t is maintained here for complete moments.

[14] The Nth normalized moment of $p(t)$, μ_N^t, is defined as the absolute Nth moment divided by the zeroth moment. The definition of a probability density function requires that the zeroth moment equal unity for a complete distribution. The Nth truncated normalized moment is the Nth truncated absolute moment divided by the zeroth truncated moment, both with the same truncation points. Because the zeroth moment is less than unity for truncated cases, the notation $\mu_N^t(t_{\min}, t_{\max})$ is maintained for the Nth truncated normalized moment.

[15] *Jawitz* [2004] derived solutions for the Nth truncated moments for several distributions commonly encountered in hydrologic applications, including the normal, lognormal, and gamma distributions. In this work, travel time and NAPL content distributions are assumed to be lognormal. The Nth truncated moment for a lognormal travel time distribution is [*Jawitz*, 2004]

$$m_N^t(t_{\min}, t_{\max}) = \frac{1}{2}\exp\left(N\mu_{\ln t} + \frac{N^2\sigma_{\ln t}^2}{2}\right) \cdot \left[\operatorname{erf}\left(\frac{\ln t_{\max} - \mu_{\ln t}}{\sigma_{\ln t}\sqrt{2}} - \frac{N\sigma_{\ln t}}{\sqrt{2}}\right) - \operatorname{erf}\left(\frac{\ln t_{\min} - \mu_{\ln t}}{\sigma_{\ln t}\sqrt{2}} - \frac{N\sigma_{\ln t}}{\sqrt{2}}\right)\right] \tag{4}$$

This equation reduces to the familiar complete distribution moments [*Aitchison and Brown*, 1957] when $t_{\min} = 0$ and $t_{\max} = \infty$:

$$m_N^t = \exp\left(N\mu_{\ln t} + N^2\sigma_{\ln t}^2/2\right) \tag{5}$$

Thus the error function terms in equation (4) are correction factors that account for truncation.

3.2. Spatially Variable NAPL Saturation

[16] The ratio of the volume of NAPL contaminants to the pore volume is defined as the NAPL saturation. Following *Jawitz et al.* [2003a], three spatially descriptive definitions of NAPL saturation are distinguished: (1) local or point saturation, S_N, (2) average saturation for the entire domain, $\overline{S}_N$, and (3) trajectory average saturation along a

streamline, $\hat{S}_N$. The spatial variability of the trajectory average NAPL content, $\hat{S} = \hat{S}_N\,\eta/\theta$ (where η is the porosity and θ is the volumetric water content), rather than $\hat{S}_N$, is described here because the latter exhibits a range of [0,1] while the range for the former is $[0, \infty)$, which is consistent with the common probability distributions, such as lognormal and gamma, that may be used to characterize the heterogeneity of this parameter.

[17] The effects of spatially variable NAPL content were investigated within the framework of correlations between $\hat{S}$ and travel time. The motivations and limitations of this approach have been described by several authors [*Berglund*, 1997; *Cvetkovic et al.*, 1998; *Jawitz et al.*, 2003a]. Conceptual arguments for a link between these parameters may be illustrated with the example of a negative correlation between $\hat{S}_N$ and t, which implies higher NAPL contents in stream tubes with shorter travel times. This conceptual model is consistent with experimental observations [e.g., *Kueper et al.*, 1993] of preferential DNAPL migration through coarse-grained media, which would be expected to translate to higher velocities (and shorter travel times). Such general models are convenient for mathematical manipulations (such as those presented here) and numerical simulations, but it is important to emphasize that concrete evidence for general models of correlations is lacking.

[18] The general correlation model used here assumes a linear relationship between the logarithms of NAPL content and travel time:

$$\ln \hat{S} = \ln a + b \ln t \tag{6}$$

where a is a constant that relates the means of t and $\hat{S}$, and b is the strength of correlation. An uncorrelated component may also be included in (6), implying that the description of $\hat{S}$ would involve two pdfs, $p(t)$ and the distribution characterizing the uncorrelated component [see *Cvetkovic et al.*, 1998; *Jawitz et al.*, 2003a]. However, only perfect correlation was considered here, which means that the $\hat{S}$ distribution is either homogeneous ($b = 0$) or increases or decreases monotonically with t ($b \neq 0$).

[19] For lognormal t, $\hat{S}$ is also lognormal with

$$\mu_{\ln \hat{S}} = \ln a + b\mu_{\ln t} \qquad \sigma_{\ln \hat{S}} = \left(b^2\sigma^2_{\ln t}\right)^{0.5} \tag{7}$$

such that the statistics of the NAPL content distribution may be expressed deterministically in terms of the travel time distribution statistics. Note that because we consider only trajectory average values, the present analysis is independent of the location of the NAPL along the trajectory.

3.3. Reactive Travel Time Statistics

[20] Following *Jawitz et al.* [2003b], the flushing duration required to remove the NAPL from a stream tube i may be expressed in terms of the contaminant retardation factor in the stream tube:

$$R_i = 1 + \frac{\rho_N \hat{S}_{N,i}\eta}{\theta C_{f,i}} = 1 + \frac{\rho_N \hat{S}_i}{C_{f,i}} = 1 + K_{f,i}\hat{S}_i \tag{8}$$

where ρ_N is the NAPL density [ML^{-3}], $C_{f,i}$ [ML^{-3}] is the contaminant concentration in the flushing solution in stream tube i, and $K_{f,i} = \rho_N/C_{f,i}$ [L^3L^{-3}] such that the product $K_{f,i}\,\hat{S}_i$ is the ratio of the contaminant mass in the nonaqueous phase and the flushing solution for stream tube i. This retardation factor approach is most useful for equilibrium dissolution cases where $C_{f,i}$ is equal to the contaminant solubility in the flushing solution, C_s, for all stream tubes containing NAPL. Nonequilibrium cases where $C_{f,i}$ varies both temporally and between stream tubes are considered separately below. Because $K_{f,i}$ is equal for all stream tubes for equilibrium dissolution, the subscript i will be dropped from this term hereafter. The retardation factor for the entire system is $R_\Omega = 1 + K_f\,\overline{S}$, where the subscript Ω indicates a property of the total domain.

[21] The retardation factor is defined as the ratio of reactive and nonreactive travel times. The reactive travel time, τ, for a stream tube may then be expressed as $\tau_i = t_i R_i = t_i + t_i\,K_f\,\hat{S}_i$. The reactive travel time is equivalent to the flushing duration required to remove the NAPL from a stream tube. The collection of τ values for an entire domain integrates the variability in both the t and $\hat{S}$ distributions. Thus the statistics of the τ distribution may be used to describe the combined effects of aquifer hydrodynamics and NAPL spatial distribution on dissolution dynamics. Following *Jawitz et al.* [2003a], the moments of the τ distribution may be expressed in terms of the moments of the t and $\hat{S}$ distributions:

$$m^\tau_N = E\left[\tau^N\right] = E\left[\left(t + tK_f\hat{S}\right)^N\right] \tag{9}$$

where the expected value notation, $E[X^N]$, is equivalent to the Nth moment of X. As described above, t and $\hat{S}$ are here considered as correlated lognormal random variables such that expansion of (9) for $N = \{1, 2\}$ results in the following expressions for the first two moments of the τ distribution [*Jawitz et al.*, 2003a]:

$$m^\tau_1 = m^t_1 + K_f m^t_1 m^{\hat{S}}_1 \gamma \tag{10}$$

$$m^\tau_2 = m^t_2\left(1 + 2K_f m^{\hat{S}}_1\gamma^2 + K^2_f m^{\hat{S}}_2\gamma^4\right) \tag{11}$$

where $\gamma = \exp\left(\rho_{t,\hat{S}}\,\sigma_{\ln t}\,\sigma_{\ln \hat{S}}\right)$, and $\rho_{t,\hat{S}} = b\sigma_{\ln t}/\sigma_{\ln \hat{S}}$ is the correlation coefficient between t and $\hat{S}$. As described by *Jawitz et al.* [2003a], when the t and $\hat{S}$ distributions are lognormal, the resulting τ distribution is also lognormal. The τ distribution parameters, $\mu_{\ln\tau}$ and $\sigma_{\ln\tau}$, may then be calculated from (10) and (11) using (5).

[22] Dividing (10) by m^t_1 results in $R_\Omega = 1 + K_f\,\mu^{\hat{S}}_1\,\gamma$. Comparison of this relation with the expression for total retardation given above, which is based on domain average NAPL content, indicates that trajectory average and domain average NAPL contents are related as follows:

$$\mu^{\hat{S}}_1 = \frac{\overline{S}}{\gamma} \tag{12}$$

Thus, for a given contaminant mass, $\mu^{\hat{S}}_1$ may vary depending on the travel time–NAPL content correlation. For uncorrelated cases ($b = 0$), $\gamma = 1$ such that $\mu^{\hat{S}}_1 = \overline{S}$. However, for positive NAPL content–travel time correlation ($b > 0$), $\gamma > 1$ and $\mu^{\hat{S}}_1 < \overline{S}$ with the opposite effect for $b < 0$. This effect has been observed in numerical simulations where negative

correlations ($b < 0$) between a reactive parameter (here NAPL content) and travel time (also commonly expressed as a positive correlation between a reactive parameter and hydraulic conductivity, which has an inverse relationship with travel time) have produced greater reactive travel times than for uncorrelated cases, with the opposite trend for $b > 0$ [*Tompson*, 1993; *Jawitz et al.*, 2003a].

[23] Tracer tests measure trajectory average parameters, including reactive and nonreactive tracer mean travel times and NAPL contents determined from the corresponding R_Ω. However, in order to determine the true mass in the system, $\mu_1^{\hat{S}}$ values obtained from tracer tests must be used with (12) to determine $\overline{S}$. Trajectory average NAPL contents interpreted as $\overline{S}$ will be overestimates for $b < 0$ and underestimates for $b > 0$ [*Jawitz et al.*, 2003a].

4. Equations for Mass Reduction and Flux Reduction Expressed as Functions of Travel Time Statistics

[24] In this section, closed form analytical relationships are developed between NAPL mass reduction, R_m, and contaminant flux reduction, R_j. These relations are expressed in terms of the moments of the nonreactive and reactive travel time distributions.

[25] Contaminant concentrations measured at monitoring or extraction wells are flux-averaged (that is, the solute mass is discharged from the porous formation into the well in proportion to the local velocity). The injection and detection mode boundary conditions for forced gradient tracer tests, from which t and $\hat{S}$ distribution statistics may be determined, are also flux-averaged (see *Demmy et al.* [1999] for a discussion of the implications of flux-averaged versus resident injection and detection modes). Therefore the contaminant mass and flux expressions presented here are formulated using flux-averaged, rather than volume-averaged, or resident concentration representations.

4.1. Preremediation Contaminant Mass

[26] The initial condition is during natural gradient water flow before flushing agents are introduced. The initial contaminant mass, M_I, in the system is the product of the pore volume and the sum of the flux-averaged concentrations of nonaqueous and dissolved aqueous phase components. Contaminant mass sorbed to the solid matrix and in the gas phase are assumed to be negligible compared to the mass in the aqueous and nonaqueous phases. The total domain pore volume can be calculated as the product of the steady state flow, Q_Ω [L^3T^{-1}], and the mean of the flux-averaged travel time distribution, $\mu_{1,\Omega}^t$. During natural gradient flow, aqueous contaminant concentrations are assumed to be at the solubility limit in stream tubes containing NAPL, and all stream tubes are assumed to initially contain NAPL. Therefore the initial contaminant mass may be expressed:

$$M_I = Q_\Omega \mu_{1,\Omega}^t \left[C_w + \mu_1^{\hat{S}} \rho_N \right] \tag{13}$$

4.2. Contaminant Mass Removed During Remediation

[27] Under the stochastic-advective framework employed here, flushing fluids delivered to an individual stream tube at $T = 0$, $x = 0$ arrive at the extraction plane when the flushing duration is equal to the stream tube travel time ($T = t_i$). When the flushing duration exceeds the stream tube reactive travel time ($T > \tau_i$), it is assumed that all of the initial NAPL has been removed (the stream tube is "clean") and the aqueous contaminant concentration is zero. The stream tube with $\tau_i = T$ is defined as the critical stream tube with $t_i = t^*$, $\hat{S}_i = \hat{S}^*$, and $\tau_i = \tau^*$ such that $T = \tau^* = t^*(1 + K_f \hat{S}^*)$. At a given T, stream tubes with $\tau_i < \tau^*$ are assumed to be clean, while those with $\tau_i > \tau^*$ will be only partially cleaned. The total mass removed during flushing, M_r, may thus be represented as the sum of the mass removed from the completely and partially cleaned portions of the domain:

$$M_r = M_c + M_{pc} \tag{14}$$

where the subscripts c and pc indicate completely and partially cleaned.

[28] The mass removed from the completely cleaned portion of the domain is the sum of the aqueous phase and NAPL components in these stream tubes:

$$M_c = Q_c \mu_{1,c}^t \left[C_w + \mu_{1,c}^{\hat{S}} \rho_N \right] \tag{15}$$

where $\mu_{1,c}^t$ and $\mu_{1,c}^{\hat{S}}$ are the means of the travel time and NAPL content distributions in the clean portion of the domain. These parameters, and the fraction of the total flow that is discharged from the clean zone, Q_c, are defined below in terms of truncated moment expressions.

[29] At any time T, the cumulative mass of contaminant removed from the partially cleaned stream tubes is the sum of three components. The first component is the mass in solution in the initially resident pore water that has been displaced from stream tubes with travel times greater than the flushing duration ($t_i > T$). The second and third components are the mass in the aqueous and flushing solutions displaced from stream tubes where the flushing duration is greater than the nonreactive travel time but less than the reactive travel time ($t_i < T < \tau_i$). The sum of these components may be expressed as

$$M_{pc} = C_w Q_{pc1} T + Q_{pc2} \left[C_w \mu_{1,pc2}^t + C_s \left(T - \mu_{1,pc2}^t \right) \right] \tag{16}$$

where the subscripts $pc1$ and $pc2$ indicate the partially cleaned stream tubes where $t_i > T$ and $t_i < T < \tau_i$, respectively. The flow Q_{pc1} may be expressed as the difference between the total flow and the flow through the stream tubes where $t_i < T$ ($Q_{pc1} = Q_\Omega - Q_{t<T}$), and the flow Q_{pc2} may be expressed as the difference between the total flow and the sum of the flow through the clean stream tubes and Q_{pc1}, ($Q_{pc2} = Q_{t<T} - Q_c$). Again, it is emphasized that (16) is only valid for equilibrium dissolution cases where $C_{f,i} = C_s$ for all stream tubes.

4.3. Mass Reduction

[30] The fractional reduction in contaminant mass is the mass removed divided by the initial mass, $R_m = M_r/M_I$. As shown in Appendix A, combining (13)–(16) and incorporating truncated moments of the nonreactive and reactive

travel time distributions results in the following expression for R_m:

$$R_m = f_{Q,c} f_{t,c} \frac{\left(1 + K_w \mu_{1,c}^{\hat{S}}\right)}{\left(1 + K_w \mu_1^{\hat{S}}\right)} + \cdot \frac{\tau^*\left(1 - f_{Q,t<T}\right)/K_w + \left(f_{Q,t<T} - f_{Q,c}\right)\left(\mu_1^t(t^*,\tau^*)/K_w + \left[\tau^* - \mu_1^t(t^*,\tau^*)\right]/K_f\right)}{\mu_{1,\Omega}^t\left(1/K_w + \mu_1^{\hat{S}}\right)} \quad (17)$$

where $f_{Q,c}$ is the fraction of the total flow that is discharged from the clean zone, $f_{t,c}$ is the ratio of the mean travel times through the clean stream tubes and the total domain, $f_{Q,t<T}$ is the fraction of the total flow that is discharged from stream tubes with travel times less than the flushing duration, and $\mu_1^t(t^*,\tau^*)$ is the mean travel time through the partially cleaned stream tubes with $t_i < T < \tau_i$. Expressions for these four parameters are provided in Appendix A in terms of truncated moments of the t and τ distributions. Also note that in (17) τ^* was substituted for T, and, analogous to K_f, $K_w = \rho_N/C_w$ [L^3L^{-3}].

[31] Equation (17) is a general expression for the fractional reduction in contaminant mass resulting from flushing-type remediation. This expression may be reduced to a final simplified form by assuming that K_w is sufficiently large that the product of K_w and NAPL content is significantly greater than one. This assumption allows (17) to be rewritten as follows:

$$R_m = f_{Q,c} f_{t,c} f_{\hat{S},c} + \frac{\left(f_{Q,t<T} - f_{Q,c}\right)\left[\tau^* - \mu_1^t(t^*,\tau^*)\right]}{K_f\, \mu_{1,\Omega}^t\, \mu_1^{\hat{S}}} \quad (18)$$

where $f_{\hat{S},c}$ is the ratio of the mean of the trajectory average NAPL contents in the clean zone and the total domain, as defined in equation (A6). The assumption of large K_w is likely to be reasonable for many recalcitrant groundwater contaminants. Consider as an example, the common NAPL contaminant trichloroethylene (TCE). The density of TCE is $\rho_N = 1.4$ g/mL and the aqueous solubility is $C_w = 1100$ mg/L, such that the product of K_w and S is more than an order of magnitude greater than 1 for $S > 0.008$.

[32] The two terms of equation (18) describe the mass reduction from the completely and partially cleaned portions of the domain. The first term is the product of the fraction of the total pore volume represented by the cleaned stream tubes and a similar ratio for NAPL content. The second term is the product of the fraction of the pore volume where the flushing duration is greater than the stream tube travel time but less than stream tube reactive travel time, and a ratio of contaminant mass in the flushing solution and the total NAPL mass. The preliminary analysis of source zone mass and flux reduction presented by *Rao and Jawitz* [2003] included only the first term.

4.4. Flux Reduction

[33] The initial mass flux, J_I, of contaminants at the extraction plane is given by

$$J_I = C_w Q_\Omega / A_\Omega \quad (19)$$

where A_Ω is the area within the extraction plane that encompasses the source zone. Postremediation conditions are here defined to be after all solubility enhancement effects from flushing fluids have been displaced from the system (either by forced gradient or natural gradient water flushing), such that dissolved mass is eluted at C_w from the stream tubes that are not completely clean. The final, postremediation mass flux, J_F, is then defined as

$$J_F = C_w (Q_\Omega - Q_c)/A_\Omega \quad (20)$$

The fractional reduction in contaminant mass flux ($R_j = 1 - J_F/J_I$), may then be expressed as

$$R_j = \frac{Q_c}{Q_\Omega} = f_{Q,c} \quad (21)$$

4.5. NAPL Content Correlated to Travel Time

[34] The NAPL content parameters in (17), (18) and (21), $\hat{S}^*$, $\mu_1^{\hat{S}}$ and $\mu_1^{\hat{S}}$ ($\hat{S}_{\min}$, $\hat{S}_{\max}$), each may be expressed in terms of travel time statistics as follows. First, the assumed relationship between NAPL content and travel time described by (6) explicitly relates $\hat{S}^* = a(t^*)^b$. Second, $\mu_1^{\hat{S}}$ may be evaluated directly from (5) using the NAPL content distribution parameters (determined from $\mu_{\ln t}$, $\sigma_{\ln t}$, a, and b using equation (7)). Third, (6) indicates that the $\hat{S}$ distribution is either homogeneous or monotonically increases or decreases with t. Therefore, for a positive correlation between t and $\hat{S}$ ($b > 0$), the lower and upper limits of the NAPL content distribution in the cleaned stream tubes are $S_{\min} = 0$ and $S_{\max} = \hat{S}^*$ such that the truncated first normalized moment of the NAPL content distribution in the cleaned zone is $\mu_1^{\hat{S}}$ (0, $\hat{S}^*$). For negatively correlated cases, this value is expressed as $\mu_1^{\hat{S}}$ ($\hat{S}^*$, ∞), and for $b = 0$ NAPL content is assumed to be homogeneous ($f_{\hat{S},c} = 1$).

[35] Thus R_m and R_j are functions of the following travel time parameters only: t^*, $\mu_{\ln t}$, $\sigma_{\ln t}$, a, and b. For a given travel time distribution and associated correlated NAPL content distribution, the latter four parameters are constants. Therefore R_m and R_j are each functions of a single variable, t^*, resulting in a direct analytical relationship between source zone mass reduction and flux reduction.

5. Enhanced Dissolution Breakthrough Curves

5.1. Equilibrium Dissolution

[36] Equation (18) may be used to determine cumulative mass removed as a function of time, but estimates of flux-averaged concentration with time (i.e., breakthrough curves, BTCs) must be determined separately. For equilibrium conditions, the NAPL concentration in the flushing solution for a given stream tube i may be expressed as a function of flushing duration T as follows:

$$C_{f,i}(T) = \begin{cases} C_w, & 0 < T < t_i \\ C_s, & t_i < T < \tau_i \\ 0, & \tau_i < T \end{cases} \quad (22)$$

The flux-averaged concentration for all stream tubes is then the product of C_w and the fraction of the flow from stream tubes with travel times greater than T ($1 - f_{Q,t<T}$), plus the product of C_s and the fraction of the flow from stream tubes

with travel times less than T but reactive travel times greater than T ($f_{Q,t<T} - f_{Q,c}$):

$$C_f(T) = C_w\left[1 - f_{Q,t<T}\right] + C_s\left[f_{Q,t<T} - f_{Q,c}\right] \tag{23}$$

[37] The cumulative mass removal, M_r, may be evaluated as a function of T by numerically integrating (23) and R_m is then determined as above by dividing M_r by M_I (determined from equation (13)). Note that this method for determining R_m produces identical results as the analytical solution (18).

5.2. Rate-Limited Dissolution

[38] Following *Cvetkovic and Dagan* [1994] and *Berglund* [1997], the equations for advection-only transport in a stream tube with a first-order mass transfer dissolution model may be written

$$\frac{\partial C_f}{\partial T} + \frac{\partial C_f}{\partial t} = -\frac{\rho_N \partial \hat{S}}{\partial T} \qquad \frac{\rho_N \partial \hat{S}}{\partial T} = -k\hat{S}\left(C_s - C_f\right) \tag{24}$$

where k [$L^3L^{-3}T^{-1}$] is a mass transfer coefficient. In this model, the effective rate parameter, $k\,\hat{S}$, is assumed to be a linear function of NAPL content. The solution to equation (24) is [*Berglund*, 1997]

$$C_{f,i}(T) = \begin{cases} C_w, & 0 < T < t_i \\ C_s\left[1 - \dfrac{\exp[k(T - t_i)/K_s]}{\exp\left[k\hat{S}_i t_i\right] + \exp[k(T - t_i)/K_s] - 1}\right], & T > t_i \end{cases} \tag{25}$$

where $K_s = \rho_N/C_s$. Thus, for nonequilibrium conditions $C_{f,i}$ is a function of residence time such that each stream tube may reflect a different C_f value at each time. Following *Berglund* [1997], (25) may be converted to dimensionless form by normalizing t, T, and $\hat{S}$ by a characteristic time (here mean travel time, μ_1^t) and incorporating the dimensionless mass transfer coefficient $k' = k\mu_1^t/K_s$. As noted by *Berglund* [1997], k' is equivalent to a ratio of the timescales of advection and mass transfer and is analogous to Damkohler number (normalized to C_s).

[39] The flux-averaged concentration for all stream tubes may be determined analogous to (23):

$$C_f(T) = C_w\left[1 - f_{Q,t<T}\right] + \int_0^T C_{f,i}(T)p(t)dt \tag{26}$$

where the second term, which must be evaluated numerically, is the flow-weighted sum of $C_{f,i}$ from the stream tubes with $t_i < T$. The cumulative mass removal may be evaluated as a function of T by numerically integrating (26) as $M_r(T) = \int C_f\,(T)dT$. Mass reduction as a function of T is then determined as above ($R_m(T) = M_r(T)/M_I$).

[40] As described by (21), reduction in contaminant flux is equivalent to the fraction of the total flow that is contributed from stream tubes that have been cleaned. For nonequilibrium dissolution cases, this quantity must be determined numerically by comparing $M_{r,i}(T)$ to $M_{I,i}$ for each stream tube. Thus reduction in contaminant flux ($R_j = 1 - J_F/J_I$) for nonequilibrium dissolution cases may be expressed as

$$R_j(T) = 1 - \frac{\sum p(t)dt|_{M_{r,i}(T)<M_{I,i}}}{\sum p(t)dt} \tag{27}$$

where the second term represents the contribution of flow from stream tubes that have not yet been cleaned.

6. Results

[41] The following factors may affect contaminant elution behavior during enhanced dissolution flushing-type remediation: porous media heterogeneity, flow path heterogeneity (e.g., well configurations), NAPL spatial distribution, and dissolution kinetics. The combined effects of the first two of these factors may be quantified in the travel time distribution. All four effects are captured by the reactive travel time distribution. Thus it is this distribution that is most important in determining the dynamics of contaminant elution, and the reduction in contaminant flux that results from a given reduction in contaminant mass.

[42] The impacts of nonreactive and reactive travel time distribution variability and rate-limited dissolution kinetics on contaminant elution are explored here in two contexts: mass reduction with time (characterized by BTCs) and flux reduction with mass reduction. Contaminant BTCs were generated analytically from (23) and numerically from (26) for equilibrium and nonequilibrium dissolution cases, respectively. Relationships between contaminant mass and flux are presented here using mass reduction/flux reduction diagrams of the type introduced by *Rao and Jawitz* [2003] where R_j is plotted as a function of R_m (i.e., $R_j(R_m)$). The mass and flux reduction terms were determined analytically from (18) and (21) and numerically from (26) and (27) for equilibrium and nonequilibrium cases, respectively. Note that when equilibrium conditions are assumed, numerical integration of (26) and (27) produces results identical to the analytical solutions.

6.1. Equilibrium Dissolution

[43] The importance of the reactive travel time distribution is demonstrated here by considering cases where different combinations of travel time and NAPL content distribution parameters are used to create the same τ distribution. Three cases are presented where K_f and $\overline{S}$ were held constant, but travel time variance, NAPL content variance, and correlation between travel time and NAPL content were varied in seven different combinations to create three different reactive travel time distributions (Table 1). Equations (10) and (11) were used to relate the parameters of these distributions. A value of $K_f = 100$ was used here, corresponding to DNAPL density $\rho_N = 1.4$ g/cm^3 and flushing solution enhanced solubility $C_f = 14{,}000$ mg/L. A domain average NAPL content $\overline{S} = 0.03$ was assumed, which is within the range of values reported from several recent field studies [e.g., *Rao et al.*, 1997; *Jawitz et al.*, 1998b, 2000; *Brooks et al.*, 2002; *Meinardus et al.*, 2002]. Note that because travel time is considered in dimensionless form (pore volume, PV = T/μ_1^t) the results here are independent of travel time mean.

[44] For case 1, $\sigma_{\ln t}$ was varied with a homogeneous NAPL content distribution to define three τ distributions. In

Table 1. Travel Time and NAPL Content Distribution Parameters[a]

Variable Parameter	$\sigma_{\ln t}$	$\sigma_{\ln \hat{S}}$	b	$\sigma_{\ln \tau}$
Case 1: $\sigma_{\ln t}$	0.2/0.6/1.0	0	0	0.2/0.6/1.0
Case 2: $\sigma_{\ln \hat{S}}$	0.5	0.44/1.05	0	0.6/1.0
Case 3: b	0.8	0.272/0.252	−0.34/+0.315	0.6/1.0

[a]The following parameters were held constant: $\mu_1{}^t = 1$, $K_f = 100$, and $\overline{S} = 0.03$.

case 2, a midrange travel time variance was combined with two values of $\sigma_{\ln \hat{S}}$ and no correlation between travel time and NAPL content. A relatively high travel time variance was selected for case 3, in combination with both positively and negatively correlated NAPL content distributions. The parameter combinations for cases 2 and 3 were selected to reproduce the latter two τ distributions from case 1. As described by (12), for a fixed $\overline{S}$ value, trajectory average NAPL content varies for correlated cases. For the positively and negatively correlated cases listed in Table 1, the corresponding $\mu_1^{\hat{S}}$ values are 0.025 and 0.037, respectively.

6.1.1. Uncorrelated Cases

[45] The BTCs resulting from the three τ distributions from Table 1 are shown in Figure 1a. Mass reduction, determined by numerically integrating the BTCs, is shown in Figure 1b. The BTCs are shown in dimensionless form where relative concentration, $C_f(T)/C_s$, is plotted as a function of PV. Two primary points are illustrated in Figure 1. First, for uncorrelated cases the BTC shapes are a function only of $\sigma_{\ln \tau}$, regardless of the combination of $\sigma_{\ln t}$ and $\sigma_{\ln \hat{S}}$ values used to define the reactive travel time distribution. Thus the case 1 and 2 parameter values listed in Table 1 for $\sigma_{\ln \tau} = \{0.6,1.0\}$ are only a subset of the infinite set that could have been used to generate the corresponding BTCs shown in Figure 1. Second, increasing the reactive travel time variance causes contaminant elution BTCs to be more dispersed (Figure 1a) such that the time required to remove a given fraction of the total contaminant mass also increases (Figure 1b). Thus source zone longevity and contaminant BTC spreading are enhanced with increasing nonreactive travel time variance or NAPL content heterogeneity.

[46] The effects of partial removal of the source zone mass on the down-gradient mass flux are shown as a function of reactive travel time variability in Figure 2. As with dissolution BTCs, the shapes of the resulting $R_j(R_m)$ relationships are sensitive to $\sigma_{\ln \tau}$, which may result from different combinations of $\sigma_{\ln t}$ and $\sigma_{\ln \hat{S}}$. For low-variance cases, large reductions in mass are required to effect any appreciable reductions in mass flux. These scenarios correspond to near-homogeneous porous media and NAPL content distributions such as those described by *Sale and McWhorter* [2001]. As τ distribution variance increases, the $R_j(R_m)$ relationship becomes more favorable, meaning that lower mass reductions are required to achieve given flux reductions.

[47] Connecting the $R_j(R_m)$ curves in Figure 2 are tie lines of equal flushing duration: $T = \{0.8,2,4,12\}$ PV. These tie lines show that for relatively short flushing durations ($T < 2$ PV for the K_f and $\overline{S}$ values used here), the range of flux reductions for different τ distribution variances is much greater than the range of mass reductions. For moderate or longer flushing durations (here $T > \sim 4$ PV), the trend is reversed where the range of flux reduction values is much greater than the range for mass reduction. Remediation of low-$\sigma_{\ln \tau}$ systems with short flushing durations will result in minimal reductions in flux, even though significant reductions in mass may be achieved. If $\sigma_{\ln \tau}$ is known to be high, then short-duration flushing may be a highly efficient means of obtaining large reductions in contaminant flux (although contaminant mass reductions will be relatively low). However, it is suggested that for cases where the τ distribution variance is subject to significant uncertainty (i.e., most contaminated sites), longer flushing durations should be pursued to overcome the risk of achieving only minimal flux reductions from short-duration flushing.

6.1.2. Empirical Description of $R_j(R_m)$

[48] As $\sigma_{\ln \tau}$ increases, the $R_j(R_m)$ curves become decreasingly convex, approach 1:1 linearity, and then become increasingly concave. Shapes of this nature may be described empirically using a power function, as suggested by *Rao et al.* [2001]. However, it was found that a power function fit to the curves shown in Figure 2 was satisfactory only for those on the right-hand side of the 1:1 line (i.e., $\sigma_{\ln \tau} < \sim 0.7$). The

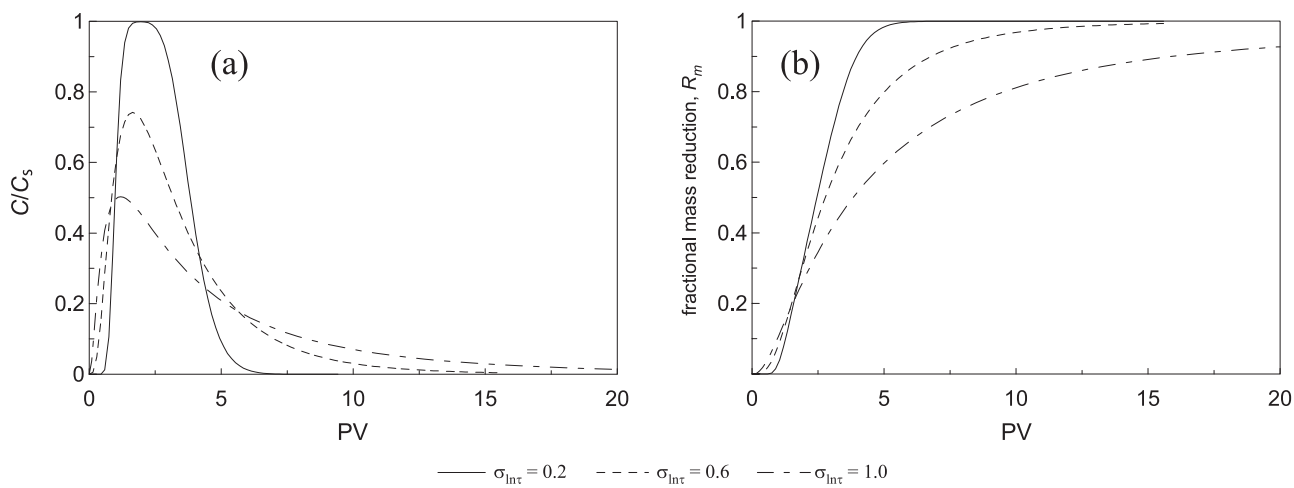

Figure 1. (a) Enhanced dissolution BTCs and (b) fractional reduction in contaminant mass calculated from equation (23) for the three cases detailed in Table 1.

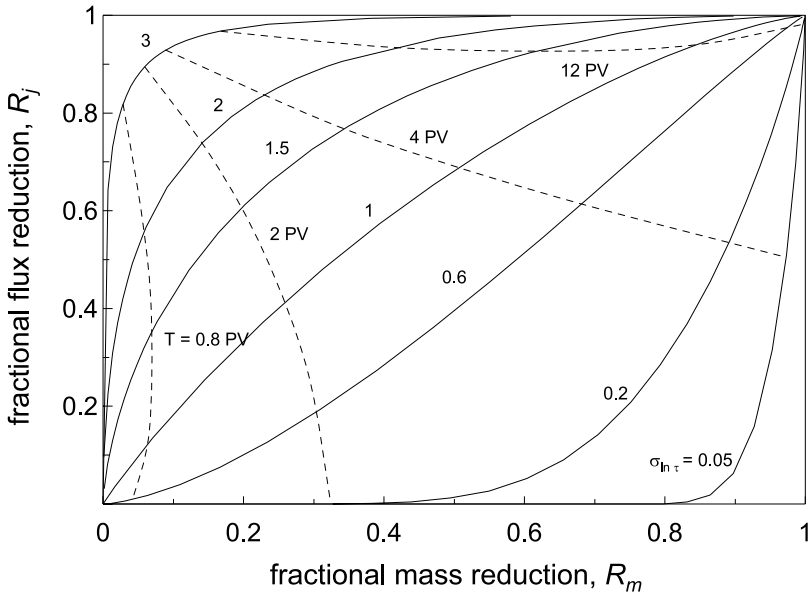

Figure 2. Reduction in contaminant flux as a function of reduction in source zone mass (solid lines) for $\sigma_{\ln\tau} = \{0.05,0.2,0.6,1.0,1.5,2.0,3.0\}$. Dashed lines are tie lines for flushing durations $T = \{0.8,2,4,12\}$ pore volumes (PV). Note that $K_f = 100$ and $\mu_{1,\hat{S}} = 0.03$.

following functions were found to provide excellent fits ($r^2 > 0.99$) to the curves shown in Figure 2:

$$R_j = \begin{cases} (R_m)^{1/\alpha}, & \sigma_{\ln\tau} \le 0.7 \\ \dfrac{R_m + \beta R_m}{1 + \beta R_m}, & \sigma_{\ln\tau} > 0.7 \end{cases} \tag{28}$$

where the empirical coefficients may be related to $\sigma_{\ln\tau}$ as follows: $\alpha = 1.31(\sigma_{\ln\tau})^{1.22}$ and $\beta = 1.03(\sigma_{\ln\tau})^{4.50}$ (also with $r^2 > 0.99$).

[49] *Correlated cases*. Travel time–NAPL content correlations had relatively minor effects on both BTCs and $R_j(R_m)$, such that the contaminant removal dynamics were still dominated by $\sigma_{\ln\tau}$. Different combinations of $\sigma_{\ln t}$, $\sigma_{\ln \hat{s}}$, and b that produce the same $\sigma_{\ln\tau}$ value were found to result in nearly identical BTCs and $R_j(R_m)$ relationships. For negative travel time–NAPL content correlations ($b < 0$), higher NAPL contents are located in stream tubes with shorter travel times, resulting in more mass elution at early times compared to uncorrelated cases. However, because these stream tubes contain more mass than for uncorrelated cases they are not cleaned as rapidly and the net effect for $b < 0$ is a slightly less favorable $R_j(R_m)$ relationship than for $b = 0$. Positively correlated cases have opposite trends with higher NAPL contents located in streamlines with longer travel times, less rapid early mass removal but more favorable $R_j(R_m)$. For example, the $R_j(R_m)$ curves from the correlated case 3 in Table 1 were assumed to be from uncorrelated cases and fit with (28) (not shown). The resulting uncorrelated equivalent $\sigma_{\ln\tau} = 0.58$ and 1.04 for $b < 0$ and $b > 0$, respectively (compared to $\sigma_{\ln\tau} = 0.6$ and 1.0 for the actual $b = 0$ cases). Thus it is emphasized that while minor differences were observed between the $b = 0$ and $b \neq 0$ cases, these effects were less significant than the effects of varying $\sigma_{\ln\tau}$, such that dissolution dynamics were primarily controlled by the latter parameter.

[50] Finally, it is noted from examination of (18) that the product $K_f\,\mu_1^{\hat{S}}$ (hereafter referred to as λ) also affects R_m, which in turn affects the $R_j(R_m)$ relationship. Different combinations of K_f and $\mu_1^{\hat{S}}$ with the same product will result in the same BTCs and $R_j(R_m)$. The relative significance of λ is illustrated in Figure 3 with $\sigma_{\ln\tau} = \{0.2,1.0\}$ from case 1 (Table 1) with $\lambda = \{0.01,1.5,3,6,100\}$. Recall that Figure 2 was generated with $\lambda = 3$. Thus the $\lambda = 3$ curves for corresponding $\sigma_{\ln\tau}$ values are equivalent in Figures 2 and 3 and may be considered as a baseline for comparison to the other λ values. Cases for $\lambda = \{1.5,6\}$ are equivalent to doubling and halving, respectively, the baseline flushing solution enhanced solubility, C_f. Alternatively, these values could be viewed as halved or doubled baseline NAPL saturations, or any combination of these parameters that results in the same product, λ. The $\lambda = \{0.1,100\}$ values correspond to the extremes for which (18) becomes insensitive to changes in this parameter. As λ decreases (equivalent to increasing flushing solution solubility), the difference between t and τ diminishes. Thus $f_{Q,t<T} - f_{Q,c}$, and concomitantly the second term of (18), which represents the mass removed from partially cleaned stream tubes, approach zero with λ. Therefore cases with very low λ values are analogous to considering only completely cleaned stream tubes. Comparison of Figures 3a and 3b indicates that as system heterogeneity increases, the effect of ignoring partially cleaned stream tubes diminishes, as suggested by *Rao and Jawitz* [2003].

[51] As λ increases (equivalent to decreasing flushing solution solubility), the flushing duration required to achieve a given mass or flux reduction also increases. For example, achieving 80% mass reduction for the $\sigma_{\ln\tau} = 0.2$ and 1.0 cases requires flushing {1.4,2.7,4.5,8.0,150} and {3.8,6.8,9.6,15,210} PVs (increasing with λ), respectively. As λ increases, individual stream tubes are cleaned less efficiently and $R_j(R_m)$ becomes less favorable as a higher mass removal percentage is required to effect a given flux

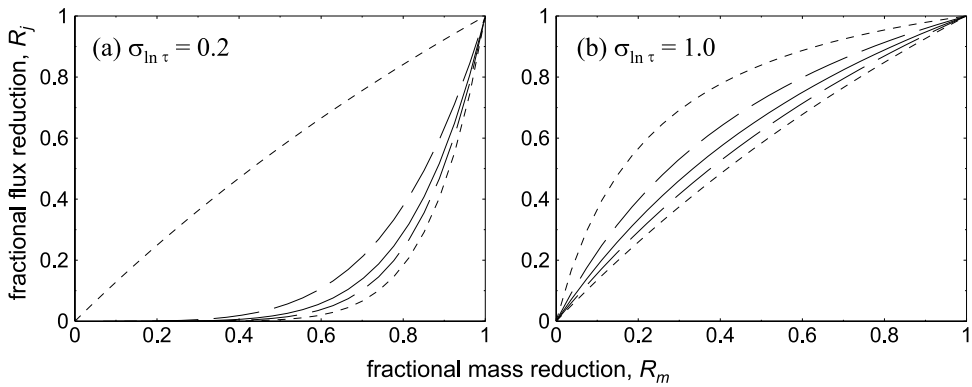

Figure 3. $R_j(R_m)$ relationship for $\sigma_{\ln\tau}$ = (a) 0.2 and (b) 1.0, with $\lambda = \{0.01,1.5,3,6,100\}$, increasing from left to right (i.e., more favorable to less favorable). Curves for $\lambda = 3$ (solid lines) are equivalent to those in Figure 2 for corresponding $\sigma_{\ln\tau}$ values.

reduction (Figure 3). Thus increasing λ has a similar effect on dissolution dynamics as decreasing $\sigma_{\ln\tau}$ (with the converse also true).

6.2. Nonequilibrium Dissolution

[52] The effects of nonequilibrium dissolution on BTCs are illustrated in Figure 4a for $\sigma_{\ln\tau} = 0.6$ (from case 1: homogeneous $\hat{S}$) for $k' = \{0.1,0.5,1.0\}$. Nonequilibrium effects are reduced as k' increases, such that equilibrium conditions are approached for $k' > \sim 10$. Decreasing k' values result in more elongated BTCs that require longer flushing durations for mass removal. These results are consistent with those of *Berglund* [1997], and the reader is referred to this study for further exploration of nonequilibrium effects on BTCs. Figures 4b and 4c illustrate nonequilibrium effects on $R_j(R_m)$ for the same range of k' values for $\sigma_{\ln\tau} = 0.6$ and 1.0 (again from case 1), respectively. Increasing rate limitations (i.e., decreasing k') result in less favorable $R_j(R_m)$ relationships. Under nonequilibrium conditions, stream tubes are cleaned less efficiently than for equilibrium cases. This effect is exacerbated by the assumption of (24) that the rate constant decreases with NAPL content. Thus rate-limited dissolution processes require longer flushing durations and result in lower flux reductions than equilibrium systems for a given mass removal.

[53] The $R_j(R_m)$ curves for the rate-limited cases in Figures 4b and 4c were not as well fit by the empirical relationship (28) ($r^2 \sim 0.9$) as the equilibrium cases. However, the equivalent $\sigma_{\ln\tau}$ values from these fits are reported here to provide a measure of the degree of change in an equilibrium case $R_j(R_m)$ that results from nonequilibrium effects. The equivalent $\sigma_{\ln\tau}$ values for the rate-limited cases were $\{0.07,0.2,0.3\}$ and $\{0.2,0.6,0.7\}$ in order of increasing k' for $\sigma_{\ln\tau} = 0.6$ and 1.0, respectively.

7. Discussion

[54] Approaches for extending the above results to increasingly complex scenarios are discussed below. Example scenarios described include multimodal travel time and NAPL content distributions and aged sites.

7.1. Multimodal Distributions

[55] For more complex hydrogeologic settings, unimodal descriptions of travel time and NAPL spatial distributions are likely to be inadequate. For example, *Jawitz et al.* [2003a, 2003b] showed that bimodal travel time distributions were necessary to model nonreactive tracer transport at three field sites. The superposition of pdfs is a convenient means of creating multimodal distributions that are consistent with the shapes of observed BTCs. For example, a bimodal distribution may be created from the superposition of two pdfs: $f(t) = (1 - F)p_1(t) + Fp_2(t)$, where $(1 - F)$ and F represent the fractional contributions of distributions 1 and 2, respectively. The moments of the multimodal distribution may be determined from an analogous superposition relationship: $m_N^t = (1 - F)m_N^{t,1} + Fm_N^{t,2}$. Note that either the nonreactive travel time or NAPL content distribution may

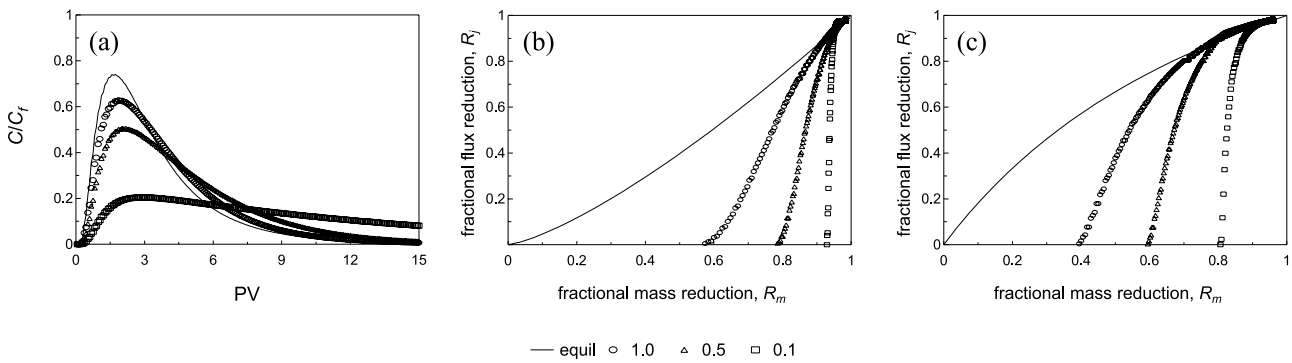

Figure 4. Nonequilibrium effects on dissolution dynamics for homogeneous NAPL content with $k' = \{1,0.5,0.1\}$: (a) comparison of BTCs for $\sigma_{\ln\tau} = 0.6$, (b) $R_j(R_m)$ for $\sigma_{\ln\tau} = 0.6$, and (c) $R_j(R_m)$ for $\sigma_{\ln\tau} = 1.0$.

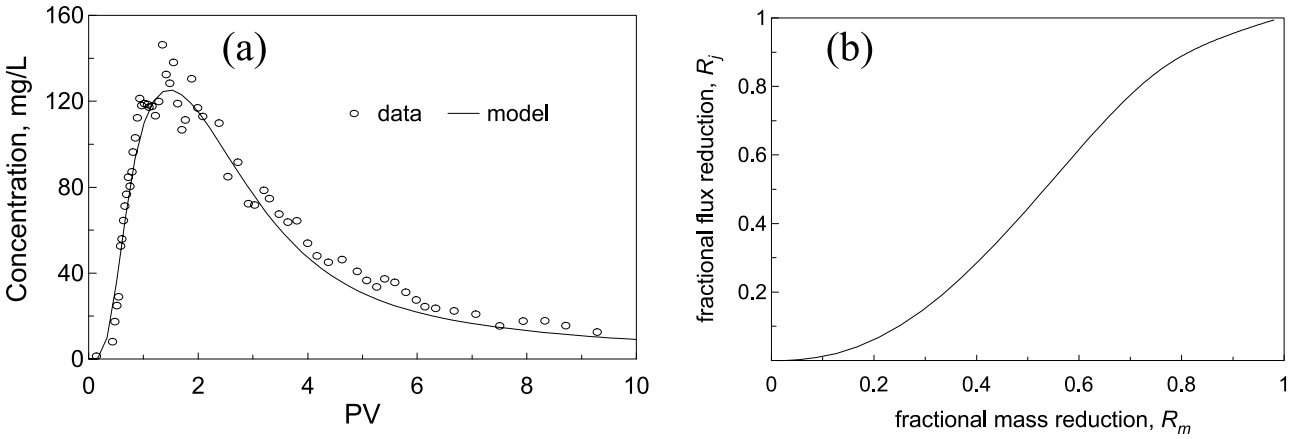

Figure 5. (a) Field dissolution data [from *Jawitz et al.*, 1998b] compared to equilibrium solution determined from (23) with a bimodal travel time distribution and homogeneous NAPL content. (b) $R_f(R_m)$ based on model parameters.

be multimodal, resulting in a similarly multimodal reactive travel time distribution. The τ distribution moments may then be determined from superposition expansions of (10) and (11), and BTCs and $R_f(R_m)$ may then be determined as described above. For example, if both travel time and NAPL content are assumed to be bimodal, (10) may be expanded as $m_1^{\tau} = (1 - F)(m_1^{t,1} + K_f\, m_1^{t,1}\, m_1^{S,1}) + F\,(m_1^{t,2} + K_f\, m_1^{t,2}\, m_1^{S,2})$. Note that this formulation assumes that travel time and NAPL content distributions 1 are contiguous, with no overlap with similarly contiguous t and $\hat{S}$ distributions 2. More complex scenarios (such as discontiguous multimodal distributions) may be pursued with the analytical approach presented here, but are beyond the scope of the present study.

[56] A brief example is presented from a field-scale in situ flushing NAPL remediation experiment performed at Hill Air Force Base (AFB), UT described by *Jawitz et al.* [1998b]. *Jawitz et al.* [2003a] found that the nonreactive travel time distribution at this site was well represented by the superposition of two lognormal distributions ($\mu_{\ln t,1} = -0.40$, $\sigma_{\ln t,1} = 0.44$, $\mu_{\ln t,2} = 0.50$, $\sigma_{\ln t,2} = 0.70$ (all in units of PV), and $F = 0.19$) with lognormal NAPL content distribution parameters $\mu_{\ln \hat{S}} = -2.81$ and $\sigma_{\ln \hat{S}} = 0.029$. On the basis of the low variability in the $\hat{S}$ distribution measured at this site, *Jawitz et al.* [2003b] assumed that NAPL content was homogeneous and were able to accurately predict the NAPL dissolution process (i.e., BTCs) by considering only travel time variability and rate-limited dissolution effects. Furthermore, these authors concluded that the microemulsion flushing technology implemented at this site was only weakly rate-limited, such that dissolution dynamics were controlled primarily by travel time variability. Therefore the equilibrium expression (23) was used here to predict the dissolution BTC of *n*-undecane, which was the most prevalent constituent of the complex multicomponent NAPL found at this site and was also representative of the observed behavior of the other compounds. The dissolution was predicted using the measured t distribution parameters, $\mu_1^S = 0.06$ [*Jawitz et al.*, 1998b] and $K_f = 53$ (based on *n*-undecane $C_f = 155$ mg/L [*Jawitz et al.*, 2003b] and mass scaled to the observed mass recovery). The BTC determined from (23) is compared to the measured data in Figure 5a. The close agreement supports the model results of *Jawitz et al.* [2003b], and indicates that accounting for the field-scale hydrodynamic heterogeneity (manifested in the travel time variability) enabled accurate prediction of the dissolution behavior.

[57] As discussed above, the performance evaluation for this experiment emphasized mass reduction, with no measurements of flux reduction. However, using (21) and the integral of (23), a mass reduction/flux reduction relationship can be estimated for this site (Figure 5b). Note that this bimodal τ distribution is not lognormal, but best fit lognormal parameters may be determined from the first two moments and (7), resulting in an equivalent $\sigma_{\ln\tau} = 0.81$. Figure 5b is generally consistent with expectations for this value based on Figure 2, except that the bimodal nature of the t (and therefore τ) distribution resulted in a more sigmoidal shape. The mass removal effectiveness for this site was estimated to be between 70% and 90% (depending on the characterization method), resulting in flux reduction estimates of 80% to 95% (Figure 5b). For microemulsion flushing, the mole fractions of the NAPL constituents did not change considerably during dissolution [*Jawitz et al.*, 1998b, 2003b]; therefore dynamic Raoult's Law considerations for multicomponent dissolution were not considered. However, it is emphasized that these effects should be incorporated when estimating mass and flux reduction from multicomponent mixtures for processes that are subject to selective solubilization (such as aqueous or cosolvent-enhanced dissolution).

[58] Finally, note that *Jawitz et al.* [2003a] used similar multimodal expressions to characterize the fraction of the stream tubes captured at the extraction plane that are contaminated, f_c. It is emphasized that the analytical approaches presented in this work apply to only the contaminated stream tubes, but extension to larger domains that also encompass uncontaminated stream tubes would simply involve scaling by f_c.

7.2. Aged Sites

[59] The analyses presented here rely on the concept of reactive travel time, which integrates nonreactive travel time (which itself couples the effects of well configuration and

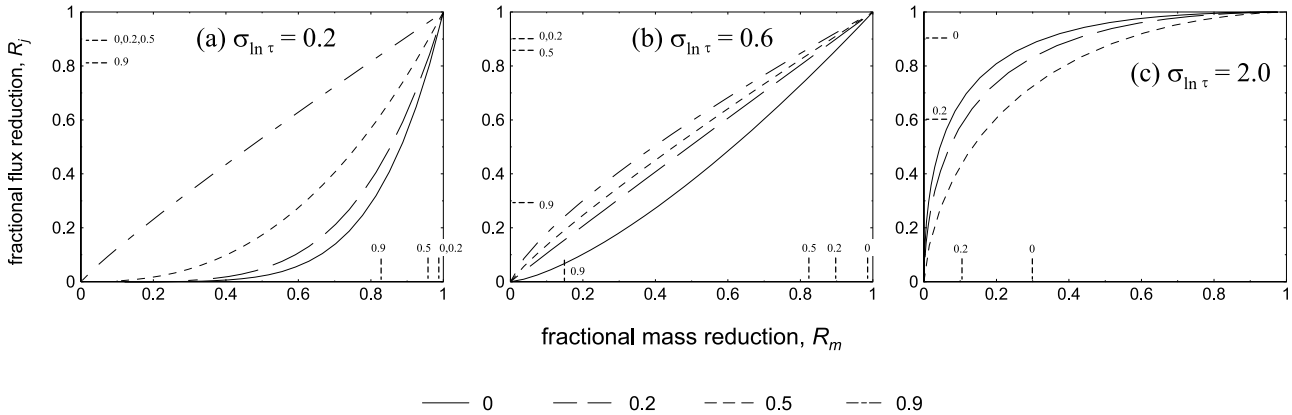

Figure 6. Aging effects on $R_j(R_m)$, for remediation with $\lambda = 3$, following source depletion by natural gradient groundwater flow for durations equivalent to $R_m = \{0,0.2,0.5,0.9\}$ for (a) $\sigma_{\ln\tau} = 0.2$, (b) $\sigma_{\ln\tau} = 0.6$, and (c) $\sigma_{\ln\tau} = 2.0$ ($R_m = 0.9$ not shown). Dashed lines on axes indicate R_m and R_j values required to reduce flux to aquifer attenuation capacity (assumed to be 10% of flux for $R_m = 0$ case) for indicated ages.

porous media heterogeneity) and a reaction parameter (here, NAPL content). The nonreactive travel time distribution is considered to be an intrinsic property that is temporally invariant and insensitive to minor effects such as relative permeability changing with NAPL content. However, the NAPL content distribution (and therefore the τ distribution) may change as mass is removed from the system. For a homogeneous τ distribution, mass is removed at equal rates from all stream tubes and the $\hat{S}$ distribution remains essentially unchanged until virtually all of the mass has been removed, which is reflected in a highly unfavorable $R_j(R_m)$ curve. Conversely, in cases with higher τ distribution variances, stream tubes with lower τ values (i.e., shorter reactive travel times resulting from either higher velocities or lower NAPL contents) are cleaned preferentially. The τ distribution therefore changes continuously during dissolution.

[60] It is emphasized that a temporally variable τ distribution connotes that the predicted remediation performance is a function of when a site is characterized. An effective parameter, $\sigma_{\ln\tau,e}$, is therefore defined to describe the shape of the τ distribution at the time of measurement or characterization, as differentiated from the initial or original $\sigma_{\ln\tau}$. Predictions of future dissolution (enhanced or aqueous) behavior are therefore predicated on when $\sigma_{\ln\tau,e}$ is measured or characterized. The time elapsed since the contamination event (site age) is quantified here in terms of the fraction of the original mass that has been removed from the contaminant source zone. This mass may be found down gradient in the groundwater plume, or it may have undergone biotic or abiotic transformations to other compounds. Site age is also reported as the number of PVs of water that would have to be displaced through the source zone to result in a given mass reduction.

[61] Aging effects on $R_j(R_m)$ were evaluated numerically as follows. In this work, the initial travel time and NAPL content distributions are assumed to be described by standard statistical distributions (or superpositions thereof). However, the τ distribution that results after some period of dissolution may not be a simple transformation of the original distribution. Therefore the initial t and $\hat{S}$ distributions were discretized to represent a bundle of stream tubes (here $n = 5000$ was used to ensure that the pdfs were represented adequately). Mass reduction was determined from the following discrete analog to (18):

$$R_m = \frac{\sum t_i \hat{S}_i\big|_{\tau_i<T} + (1/K_f)\sum (T - t_i)\big|_{t_i<T<\tau_i}}{\sum t_i \hat{S}_i} \qquad (29)$$

where $K_w\,\mu_1^{\hat{S}}$, as in (18), was assumed to be much greater than one. Flux reduction was determined according to (21). Note that this formulation represents a collection of equal flux stream tubes.

[62] The effect of site age on $R_j(R_m)$ was evaluated here with three example τ distributions: $\sigma_{\ln\tau} = \{0.2,0.6,2.0\}$, with homogeneous NAPL content, $\mu_1^{\hat{S}} = 0.03$. Each case was aged by aqueous dissolution with $C_f = C_w = 100$ mg/L ($K_{f,w} = 1.4 \times 10^3$ and $\lambda = 420$) for durations sufficient to achieve $R_m = \{0.2,0.5,0.9\}$. The corresponding number of PVs of water flushing required to age to $R_m = 0.2$ were {85,90,230}, for the three cases respectively. For $R_m = 0.5$ and 0.9, these values were {210,230,1700} and {400,650}, where results for $R_m = 0.9$, $\sigma_{\ln\tau} = 2.0$ are not shown because the required number of PVs ($>10^5$) was orders of magnitude greater than for the other cases. As noted above, increasing $\sigma_{\ln\tau}$ requires longer flushing durations to achieve similar mass or flux reduction. Following aging, the NAPL remaining in each stream tube (determined from the difference between the initial value and the amount removed) was considered as the initial $\hat{S}$ distribution for a subsequent remedial flood with $K_f = 100$ ($\lambda = 3$ as above).

[63] For each initial $\sigma_{\ln\tau}$, a sequence of $R_j(R_m)$ curves is shown in Figure 6 where it was assumed that the systems were characterized with new $\sigma_{\ln\tau,e}$ values at successive ages. For the cases with initial $\sigma_{\ln\tau} = 0.2$ and 0.6, $\sigma_{\ln\tau,e}$ increased with age to {0.24,0.37,0.87} and {0.81,0.90,1.0}, respectively. For initial $\sigma_{\ln\tau} = 2.0$, $\sigma_{\ln\tau,e}$ decreased with age to {1.8,1.5}. For less heterogeneous and relatively unfavorable $R_j(R_m)$ cases, aging increases the variance of the remaining τ distribution such that $R_j(R_m)$ becomes more favorable with site age, reaching a limit near $\sigma_{\ln\tau,e} = 1.0$. For more heterogeneous and relatively favorable $R_j(R_m)$ cases, aging has the reverse effect on the remaining τ

distribution. A similar analysis with initial $\sigma_{\ln\tau} = 1.0$ (not shown) found that the $R_j(R_m)$ curves were virtually unchanged by aging. Thus, as sites age a convergence toward approximately $\sigma_{\ln\tau} = 1.0$ is indicated.

[64] It is cautioned that when considering mass and flux reduction in relative terms (such as in the $R_j(R_m)$ curves presented here), the absolute values that will determine remedial endpoints should also be kept in perspective. This is particularly so when comparing $R_j(R_m)$ curves that reflect different conditions such as K_f or initial τ distribution. Here it is assumed that the remedial target is the aquifer attenuation capacity, A, expressed in terms of contaminant flux. The curves in Figure 6 may then be appropriately compared by considering the flux reduction required to meet A, the mass reduction required to achieve this level of flux reduction, and the corresponding required flushing duration.

[65] As a site ages, the original mass is depleted and the flux is reduced according to the original $R_j(R_m)$. However, if at any intermediate time $\sigma_{\ln\tau,e}$ is characterized to create a new $R_j(R_m)$, the revised flux reduction required to meet A will be lower than the original R_j because both the mass and flux had already been depleted for some time. These effects are illustrated in Figure 6, where the R_j and R_m values required to meet A (assumed to be equal to 10% of the original flux) are indicated on the axes for different ages. For the initial conditions (i.e., age duration equivalent to $R_m = 0$), A is met with $R_j = 0.9$ and the R_m required to achieve this flux reduction decreases as $\sigma_{\ln\tau}$ increases. The apparent R_j and R_m values required to meet A decrease with age, as indicated on the axes of Figure 6. Naturally, the corresponding flushing durations for enhanced dissolution required to attain A also decreased with age. For $\sigma_{\ln\tau} = 0.2$, the required flushing durations (with $\lambda = 3$) were {5.0,4.4,3.5,2.2} PVs for increasing age (the first value is for the original condition). Equivalent values for $\sigma_{\ln\tau} = \{0.6,2.0\}$ were {7.0,6.4,5.5,2.5} and {6.9,5.2,0,0} PVs (for $\sigma_{\ln\tau} = 2.0$, $R_m = \{0.5,0.9\}$, the flux was already below A). Note that because the $R_m = 0$ curves are equivalent to those in Figure 2, these flushing durations may also be interpolated from the tie lines in Figure 6.

[66] These results may be synthesized by considering each case separately. For the weakly heterogeneous case $\sigma_{\ln\tau} = 0.2$, the original $R_j(R_m)$ curve is relatively unfavorable: achieving $R_j = \{0.50,0.90\}$ requires $R_m = \{0.90,0.98\}$. After aging until 90% of the original mass has been dissolved, $R_j(R_m)$ becomes more favorable such that $R_j = \{0.50,0.90\}$ requires only $R_m = \{0.50,0.90\}$. To achieve A (i.e., 90% reduction in the original flux) at this point requires removal of 80% of the mass remaining (which corresponds to a total removal of 98% of the original mass) (Figure 6a). For $\sigma_{\ln\tau} = 0.6$, after aging to $R_m = 0.9$, A may be achieved with the additional removal of only 15% of the mass remaining (equivalent to flushing 2.5 PV with $\lambda = 3$) (Figure 6b). For $\sigma_{\ln\tau} = 2.0$, the original flux was reduced 60% after aging to $R_m = 0.2$ (Figure 6c), and aging until $R_m = 0.5$ resulted in a reduction in the original flux of 95% (i.e., already below A).

[67] An important implication of these results is that aging combined with the effects of field-scale heterogeneities in travel time and NAPL content distributions will place many real contaminated sites in the midrange of the family of $R_j(R_m)$ curves, with near equivalent flux reduction for a given mass reduction. For example, as discussed above, $\sigma_{\ln\tau} = 0.81$ was found at a NAPL-contaminated site at Hill AFB, UT. *Jawitz et al.* [2003b] also presented data from a NAPL-contaminated site in Jacksonville, FL corresponding to $\sigma_{\ln\tau} = \{0.87,0.85\}$ for the swept volumes of two extraction wells. At sites with these levels (or higher) of field-scale heterogeneities, longer flushing durations are required to achieve a given mass reduction than at less heterogeneous sites. However, the resulting reduction in flux is greater for these more heterogeneous sites such that the flushing duration required to reach A may not be significantly different.

8. Conclusions

[68] Contaminant elution dynamics are controlled by the combined effects of dissolution kinetics and spatial variability in travel time and NAPL content. The latter two effects are manifested together in the reactive travel time distribution, enabling description of the overall system heterogeneity (including both NAPL architecture and media heterogeneity) with a single measurable parameter: $\sigma_{\ln\tau}$. Thus the variability of the reactive travel time distribution and the dissolution kinetics determine the resulting enhanced dissolution BTC and the relationship between mass reduction and flux reduction. Two approaches using truncated moments were presented to evaluate the relationship between R_m and R_j. The first is an analytical expression, while the second provides a direct solution for solute BTCs, but requires numerical integration to obtain R_m and R_j. Both approaches provide identical results and similar opportunities to explore the relative significance of and interactions between regulating parameters.

[69] Increased τ distribution variance was shown to result in increased BTC spreading and longer flushing duration to remove NAPL. However, increased τ variability also leads to more favorable relationships between mass reduction and flux reduction. Rate-limited dissolution processes require longer flushing durations and result in lower flux reductions than equilibrium systems for a given mass removal. Comparison with measured field data suggests that real field site variability combined with aging processes will lead to measurable flux reductions with even moderate mass reduction.

[70] Aquifer attenuation capacity is recommended as a remedial target for contaminant flux discharged from the source zone. However, contaminant flux and aquifer attenuation capacity data have yet to be presented for a variety of field conditions. Thus it is emphasized that criteria for determining appropriate levels of flux reduction to achieve risk management goals have yet to be broadly defined.

Appendix A

[71] Combination and simplification of (13)–(16) results in the following expression for R_m:

$$R_m = \frac{Q_c \mu^t_{1,c}\left(1 + K_w \mu^{\hat{S}}_{1,c}\right)}{Q_\Omega \mu^t_{1,\Omega}\left(1 + K_w \mu^{\hat{S}}_1\right)} + \frac{(Q_\Omega - Q_{t<T})(T/K_w) + (Q_{t<T} - Q_c)\left(\mu^t_{1,pc2}/K_w + \left(T - \mu^t_{1,pc2}\right)/K_f\right)}{Q_\Omega \mu^t_{1,\Omega}\left(1/K_w + \mu^{\hat{S}}_1\right)} \tag{A1}$$

Equation (A1) may be simplified using the following five definitions that employ truncated moments. First, the fraction of the total flow that is discharged from the clean zone is equivalent to the fraction of the flow from stream tubes with reactive travel times less than τ^*. This ratio, designated $f_{Q,c}$, is equal to the ratio of the truncated and complete zeroth moments of the flux-averaged τ distribution, $g(\tau)$:

$$f_{Q,c} = \frac{Q_c}{Q_\Omega} = \frac{\int_0^{\tau^*} g(\tau)d\tau}{\int_0^{\infty} g(\tau)d\tau} = \frac{m_0^{\tau}(0,\tau^*)}{m_0^{\tau}} \quad \text{(A2)}$$

Note that for homogeneous NAPL contents, the t and τ distributions are linearly related such that $f_{Q,c}$ may also be expressed in terms of the truncated zeroth moment of the flux-averaged t distribution for this case.

[72] Second, the fraction of the total flow that is discharged from stream tubes with travel times less than the flushing duration, $f_{Q,t<T}$, may be similarly expressed as the ratio of the truncated and complete zeroth moment for the flux-averaged travel time distribution:

$$f_{Q,t<T} = \frac{Q_{t<T}}{Q_\Omega} = \frac{\int_0^{T} p(t)dt}{\int_0^{\infty} p(t)dt} = \frac{m_0^{t}(0,T)}{m_0^{t}} \quad \text{(A3)}$$

Third, the ratio of the mean travel times through the clean stream tubes and the total domain, $f_{t,c}$, is defined:

$$f_{t,c} = \frac{\mu_{1,c}^{t}}{\mu_{1,\Omega}^{t}} = \left(\frac{\int_0^{t^*} t\,p(t)dt}{\int_0^{t^*} p(t)dt}\right)\left(\frac{\int_0^{\infty} p(t)dt}{\int_0^{\infty} tp(t)dt}\right) = \frac{\mu_1^{t}(0,t^*)}{\mu_1^{t}} \quad \text{(A4)}$$

Fourth, the mean travel time through the partially cleaned stream tubes with $t_i < T < \tau_i$ may be evaluated from the first normalized truncated moment of the flux-averaged travel time distribution for travel times greater than t^* and less than τ^*:

$$\mu_{1,pc2}^{t} = \frac{\int_{t^*}^{\tau^*} t\,p(t)dt}{\int_{t^*}^{\tau^*} p(t)dt} = \mu_1^{t}(t^*,\tau^*) \quad \text{(A5)}$$

Finally, the ratio of the mean of the trajectory average NAPL contents in the clean zone and the total domain, $f_{\hat{S},c}$, is defined analogous to (A4):

$$f_{\hat{S},c} = \frac{\mu_{1,c}^{\hat{S}}}{\mu_1^{\hat{S}}} = \frac{\mu_1^{\hat{S}}(\hat{S}_{\min},\hat{S}_{\max})}{\mu_1^{\hat{S}}} \quad \text{(A6)}$$

where the $\hat{S}$ distribution is also flux-averaged, and the values of the limits $\hat{S}_{\min}$ and $\hat{S}_{\max}$ depend on the correlation between NAPL content and t, as discussed above.

[73] Here, travel time and NAPL content were assumed to follow lognormal distributions such that (A2)–(A6) may be solved using the truncated moment expression (TME) of (4). Other statistical distributions, such as normal or gamma, may also be used to describe these parameters using the TMEs presented by *Jawitz* [2004]. However, the relationship between t, $\hat{S}$ and τ described by (10) and (11) may not be valid for other distributions.

[74] **Acknowledgments.** Michael D. Annable and Kirk Hatfield are gratefully acknowledged for helpful discussions and constructive comments. This research was supported by the Florida Agricultural Experiment Station and a grant from SERDP (Strategic Environmental Research and Development Program) and approved for publication as Journal Series R-10923.

References

Aitchison, J., and J. A. C. Brown (1957), *The Lognormal Distribution*, Cambridge Univ. Press, New York.

Berglund, S. (1997), Aquifer remediation by pumping: A model for stochastic-advective transport with nonqauoues phase liquid dissolution, *Water Resour. Res.*, *33*(4), 649–661.

Berglund, S., and A. Fiori (1997), Influence of transverse mixing on the breakthrough of sorbing solute in a heterogeneous aquifer, *Water Resour. Res.*, *33*(3), 399–406.

Bockelmann, A., T. Ptak, and G. Teutsch (2001), An analytical quantification of mass fluxes and natural attenuation rate constants at a former gasworks site, *J. Contam. Hydrol.*, *53*, 429–453.

Brooks, M. C., M. D. Annable, P. S. C. Rao, K. Hatfield, J. W. Jawitz, W. R. Wise, A. L. Wood, and C. G. Enfield (2002), Controlled release, blind tests of DNAPL characterization using partitioning tracers, *J. Contam. Hydrol.*, *59*, 187–210.

Brooks, M. C., M. D. Annable, P. S. C. Rao, K. Hatfield, J. W. Jawitz, W. R. Wise, A. L. Wood, and C. G. Enfield (2004), Controlled release, blind test of DNAPL remediation by ethanol flushing, *J. Contam. Hydrol.*, *69*, 281–297, doi:10.1016/S0169-7722 (03)00158-X.

Chrysikopoulos, C. V., K. Y. Lee, and T. C. Harmon (2000), Dissolution of a well-defined trichloroethylene pool in saturated porous media: Experimental design and aquifer characterization, *Water Resour. Res.*, *36*(7), 1687–1696.

Cirpka, O. A., and P. K. Kitanidis (2000), An advective-dispersive stream tube approach for the transfer of conservative-tracer data to reactive transport, *Water Resour. Res.*, *36*(5), 1209–1220.

Cvetkovic, V., and G. Dagan (1994), Transport of kinetically sorbing solute by steady random velocity in heterogeneous porous formations, *J. Fluid Mech.*, *265*, 189–215.

Cvetkovic, V., G. Dagan, and H. Cheng (1998), Contaminant transport in aquifers with spatially variable hydraulic and sorption properties, *Proc. R. Soc. London, Ser. A*, *454*, 2173–2207.

Demmy, G., S. Berglund, and W. Graham (1999), Injection mode implications for solute transport in porous media: Analysis in a stochastic Lagrangian framework, *Water Resour. Res.*, *35*(7), 1965–1973.

Eberhardt, C., and P. Grathwohl (2002), Time scales of organic contaminant dissolution from complex source zones: Coal tar pools vs. blobs, *J. Contam Hydrol.*, *59*(1–2), 45–66.

Falta, R. W., C. M. Lee, S. E. Brame, E. Roeder, J. T. Coates, C. Wright, A. L. Wood, and C. G. Enfield (1999), Field test of high molecular weight alcohol flushing for subsurface nonaqueous phase liquid remediation, *Water Resour. Res.*, *35*(7), 2095–2108.

Fiorenza, S. (2000), *NAPL Removal: Surfactants, Foams, and Microemulsions*, Lewis, Boca Raton, Fla.

Fountain, J. C., R. C. Starr, T. Middleton, M. Beikirch, C. Taylor, and D. Hodge (1996), A controlled field test of surfactant-enhanced aquifer remediation, *Ground Water*, *34*(5), 910–916.

Geller, J. T., and J. R. Hunt (1993), Mass-transfer from nonaqueous phase organic liquids in water-saturated porous media, *Water Resour. Res.*, *29*(4), 833–845.

Ginn, T. R. (2001), Stochastic-convective transport with nonlinear reactions and mixing: Finite streamtube ensemble formulation for multicomponent reaction systems with intra-streamtube dispersion, *J. Contam. Hydrol.*, *47*, 1–28.

Hatfield, K., M. Annable, J. H. Cho, P. S. C. Rao, and H. Klammler (2004), A direct passive method for measuring water and contaminant fluxes in porous media, *J. Contam. Hydrol.*, *75*, 155–181.

Jawitz, J. W. (2004), Moments of truncated continuous univariate distributions, *Adv. Water Resour.*, *27*(3), 269–281, doi:10.1016/j.advwatres.2003.12.002.

Jawitz, J. W., M. D. Annable, and P. S. C. Rao (1998a), Miscible fluid displacement stability in unconfined porous media: Two-dimensional flow experiments and simulations, *J. Contam. Hydrol.*, *31*, 211–230.

Jawitz, J. W., M. D. Annable, P. S. C. Rao, and R. D. Rhue (1998b), Field implementation of a Winsor type I surfactant/alcohol mixture for in situ solubilization of a complex LNAPL as a single phase microemulsion, *Environ. Sci. Technol.*, *32*(4), 523–530.

Jawitz, J. W., R. K. Sillan, M. D. Annable, P. S. C. Rao, and K. Warner (2000), In situ alcohol flushing of a DNAPL source zone at a dry cleaner site, *Environ. Sci. Technol.*, *34*(17), 3722–3729.

Jawitz, J. W., M. D. Annable, G. G. Demmy, and P. S. C. Rao (2003a), Estimating non-aqueous phase liquid spatial variability using partitioning tracer higher temporal moments, *Water Resour. Res.*, *39*(7), 1192, doi:10.1029/2002WR001309.

Jawitz, J. W., D. Dai, P. S. C. Rao, M. D. Annable, and R. D. Rhue (2003b), Rate-limited solubilization of multi-component nonaqueous phase liquids by flushing with cosolvents and surfactants: Modeling data from laboratory and field experiments, *Environ. Sci. Technol.*, *37*(9), 1983–1991, doi:10.1021/es0256921.

Jury, W. A., and K. Roth (1990), *Transfer Functions and Solute Movement Through Soil*, Springer, New York.

Klenk, I. D., and P. Grathwohl (2002), Transverse vertical dispersion in groundwater and the capillary fringe, *J. Contam. Hydrol.*, *58*, 111–128.

Kueper, B. H., D. Redman, R. C. Starr, S. Reitsma, and M. Mah (1993), A field experiment to study the behavior of tetrachloroethylene below the water-table: Spatial distribution of residual and pooled DNAPL, *Ground Water*, *31*(5), 756–766.

Lemke, L. D., L. M. Abriola, and J. R. Lang (2004), Influence of hydraulic property correlation on predicted dense nonaqueous phase liquid source zone architecture, mass recovery, and contaminant flux, *Water Resour. Res.*, *40*, W01511, doi:10.1029/2003WR001980.

Lowe, D. F., C. L. Oubre, C. H. Ward, and T. J. Simpkin (1999), *Surfactants and Cosolvents for NAPL Remediation: A Technology Practices Manual*, Lewis, Boca Raton, Fla.

Martel, R., P. J. Gelinas, and L. Saumure (1998), Aquifer washing by micellar solutions: 3 Field test at the Thouin Sand Pit (L'Assomption, Quebec, Canada), *J. Contam. Hydrol.*, *30*, 33–48.

McCray, J. E., and M. L. Brusseau (1998), Cyclodextrin-enhanced in situ flushing of multiple-component immiscible organic liquid contamination at the field scale: Mass removal effectiveness, *Environ. Sci. Technol.*, *32*(9), 1285–1293.

McWhorter, D. B., and T. C. Sale (2003), Reply to comment by P. S. C. Rao and J. W. Jawitz on "Steady state mass transfer from single-component dense nonaqueous phase liquids in uniform flow fields" by T. C. Sale and D. B. McWhorter, *Water Resour. Res.*, *39*(3), 1069, doi:10.1029/2002WR001423.

Meinardus, H. W., V. Dwarakanath, J. Ewing, G. J. Hirasaki, R. E. Jackson, M. Jin, J. S. Ginn, J. T. Londergan, C. A. Miller, and G. A. Pope (2002), Performance assessment of NAPL remediation in heterogeneous alluvium, *J. Contam. Hydrol.*, *54*, 173–193.

Parker, J. C., and E. Park (2004), Modeling field-scale dense nonaqueous phase liquid dissolution kinetics in heterogeneous aquifers, *Water Resour. Res.*, *40*(5), W05109, doi:10.1029/2003WR002807.

Rao, P. S. C., and J. W. Jawitz (2003), Comment on "Steady-state mass transfer from single-component dense non-aqueous phase liquids in uniform flow fields" by T.C. Sale and D. B. McWhorter, *Water Resour. Res.*, *39*(3), 1068, doi:10.1029/2001WR000599.

Rao, P. S. C., M. D. Annable, R. K. Sillan, D. P. Dai, K. Hatfield, W. D. Graham, A. L. Wood, and C. G. Enfield (1997), Field-scale evaluation of in situ cosolvent flushing for enhanced aquifer remediation, *Water Resour. Res.*, *33*(12), 2673–2686.

Rao, P. S. C., J. W. Jawitz, C. G. Enfield, R. W. Falta, M. D. Annable, and A. L. Wood (2001), Technology integration for contaminated site remediation: Cleanup goals and performance criteria, in *Groundwater Quality 2001: Natural and Enhanced Restoration of Groundwater Pollution, Proceedings of the 3rd International Conference, Sheffield, England, June 18–21*, edited by S. Thornton and S. Oswald, *IAHS Publ.*, *273*, 410–412.

Rivett, M. O., and S. Feenstra (2005), Dissolution of an emplaced source of DNAPL in a natural aquifer setting, *Environ. Sci. Technol.*, *39*, 447–455.

Sale, T. C., and D. B. McWhorter (2001), Steady state mass transfer from single-component dense nonaqueous phase liquids in uniform flow fields, *Water Resour. Res.*, *37*(2), 393–404.

Tompson, A. F. B. (1993), Numerical simulation of chemical migration in physically and chemically heterogeneous porous media, *Water Resour. Res.*, *29*(11), 3709–3726.

U. S. Environmental Protection Agency (USEPA) (2003), The DNAPL remediation challenge: Is there a case for source depletion?, *Rep. EPA/600/R-03/143*, Natl. Risk Manage. Res. Lab., Cincinnati, Ohio.

S. Berglund, Swedish Nuclear Fuel and Waste Management Company, P.O. Box 5864, SE-102 40 Stockholm, Sweden.

G. G. Demmy, TerraGo Technologies, 155 Woolco Drive, Marietta, GA 30062, USA.

A. D. Fure, Department of Environmental Engineering Sciences, University of Florida, Gainesville, FL 32611, USA.

J. W. Jawitz, Soil and Water Science Department, University of Florida, PO Box 110290, 2169 McCarty Hall, Gainesville, FL 32611, USA. (jawitz@ufl.edu)

P. S. C. Rao, School of Civil Engineering, Purdue University, West Lafayette, IN 47907, USA.